Isomers and Energy Landscapes of Perchlorate-Water Clusters and a Comparison to Pure Water and Sulfate-Water Clusters

Hey, John C; Smeeton, Lewis C; Oakley, Mark T; Johnston, Roy L

DOI:
10.1021/acs.jpca.6b01495

Document Version
Peer reviewed version

Citation for published version (Harvard):
Hey, JC, Smeeton, LC, Oakley, MT & Johnston, RL 2016, 'Isomers and Energy Landscapes of Perchlorate-Water Clusters and a Comparison to Pure Water and Sulfate-Water Clusters', *The Journal of Physical Chemistry A*, vol. 120, no. 23, pp. 4008-15. https://doi.org/10.1021/acs.jpca.6b01495

Isomers and Energy Landscapes of Perchlorate-Water Clusters and a Comparison to Pure Water and Sulfate-Water Clusters

John C. Hey, Lewis C. Smeeton, Mark T. Oakley and Roy L. Johnston[*]

School of Chemistry, University of Birmingham, Edgbaston, Birmingham, B15 2TT, UK

Abstract

Hydrated ions are crucially important in a wide array of environments, from biology to the atmosphere, and the presence and concentration of ions in a system can drastically alter its behavior. One way in which ions can affect systems is in their interactions with proteins. The Hofmeister series ranks ions by their ability to salt-out proteins, with kosmotropes, such as sulfate, increasing their stability and chaotropes, such as perchlorate, decreasing their stability. We study hydrated perchlorate clusters as they are strongly chaotropic and thus exhibits different properties to sulfate. In this study we simulate small hydrated perchlorate clusters using a basin-hopping geometry optimization search with empirical potentials. We compare topological features of these clusters to data from both computational and experimental studies of hydrated sulfate ions and draw some conclusions about ion effects in the Hofmeister series. We observe a patterning conferred to the water molecules within the cluster by the presence of the perchlorate ion and compare the magnitude of this effect to that observed in previous studies involving sulfate. We also investigate the influence of the overall ionic charge on the low-energy structures adopted by these clusters.

[*] E-mail: r.l.johnston@bham.ac.uk Tel: +44 121 414 7477

1. Introduction

The Hofmeister series is an ordering given to solutions of ions based on properties such as their ability to desolvate or "salt-out" proteins or their specific ion effects.[1,2] This effect was first reported in 1888 by Lewith and Hofmeister based on their work on protein solubilities.[3] The Hofmeister series is separated into kosmotropes (order-making) and chaotropes (disorder-making). Ions at opposite ends of the Hofmeister series have different effects on species in solution.[1,3–6] Kosmotropes generally increase the solubility of proteins whilst chaotropes decrease their solubility.[1] Hofmeister ions have also been shown to affect the surface interfacial properties of electrolytic solutions.[3,4,5,7] Understanding the Hofmeister series is important because its effects can be seen in many different systems including industrial processes and atmospheric chemistry as well as in biology.[8–10]

In previous work, we have studied the sulfate ion (SO_4^{2-}) solvated in a finite water cluster.[11] Sulfate is one of the most kosmotropic Hofmeister ions, while perchlorate (ClO_4^-) is one of the more chaotropic Hofmeister ions. Here, we present a study of the structures and energy landscapes of hydrated perchlorate clusters $(ClO_4^-)(H_2O)_N$, with $N \leq 50$, making comparisons with hydrated sulfate clusters and pure water clusters, in order to draw some general conclusions about the Hofmeister series.

2. Methodology

Due to the relatively large sizes and complexities of the systems under consideration we have used an empirical potential energy model and rigid bodies (i.e. with fixed bond lengths and angles) to represent the perchlorate and sulfate ions and the water molecules. Modelling the molecular entities as rigid bodies allows them to be described by angle axis

coordinates, this permits inexpensive changes to geometry, whilst avoiding the problems inherent in the Euler axis system.[12,13] Rigid body modelling also significantly reduces the computational expense, as it removes the internal degrees of freedom from the fragments and reduces the search space for global optimization.

The interaction energy (U) of the ion-water cluster was evaluated as the sum of coulombic and Lennard-Jones contributions over all pairs of interacting sites (atoms and water lone pair sites).

$$U = \sum_{i=1}^{N} \sum_{j=i+1}^{N} \left\{ \frac{q_i q_j}{r_{ij}} + 4\epsilon_{ij} \left[\left(\frac{\sigma_{ij}}{r_{ij}} \right)^{12} - \left(\frac{\sigma_{ij}}{r_{ij}} \right)^{6} \right] \right\} \quad (1)$$

where σ_{ij} and ε_{ij} are the Lennard-Jones distance and energy parameters, r_{ij} is the inter-site separation, and q_i and q_j are the charges of sites i and j, respectively.

The Lennard-Jones parameters and partial charges used for perchlorate were taken from the literature and were determined by *ab initio* LCAO MO SCF calculations.[14,15] The perchlorate ion was modelled as a rigid tetrahedral molecule with O-Cl-O bond angles of 109.5° and Cl-O bond lengths of 1.44 Å.

Sulfate was also modelled as a rigid tetrahedron with O-S-O bond angles of 109.5° and S-O bond lengths of 1.49 Å. The Lennard-Jones parameters and partial charges used for sulfate were derived using Møller–Plesset MP4SDTQ *ab initio* calculations.[11,16] The water molecules were modelled using the TIP4P potential, a rigid four-body molecule is defined with a H-O-H bond angle of 104.52°, with an oxygen lone pair site described as a pseudo-atom which

Table 1. Lennard-Jones parameters and partial charges for perchlorate, sulfate and TIP4P water.

Molecule	Atom Type	ε / kcal mol^{-1}	σ / Å	q /e
Perchlorate ClO_4^-	Cl	0.0401572	4.9	0.44
	O	0.075723	3.1	-0.35
Sulfate SO_4^{2-}	S	0.25	3.6	2.4
	O	0.25	3.2	-1.1
TIP4P H_2O	O	0.648	3.2	0
	Lone pair	0	0	-1.04
	H	0	0	0.52

carries the charge of the oxygen but which has no Lennard-Jones parameters.[17,18] This TIP4P model has been shown to replicate experimental data for bulk water whilst also being computationally inexpensive. [18,19,20,21] The Lennard-Jones parameters and partial charges for all molecules are presented in Table 1.

Low-energy minima on the potential energy surface for the perchlorate-water and sulfate-water clusters were found using the basin-hopping Monte Carlo algorithm[22,23,24] implemented in the pele[25] software package. The basin-hopping algorithm is used to obtain the putative lowest-energy structure (the global minimum, GM), to explore the potential energy landscape efficiently, and locate other low energy structures, for subsequent landscape mapping.[22,24]

The Monte Carlo geometry perturbations implemented in this study were performed in blocks of 100 moves of the same type.[26] Three move-classes have been implemented: rotations; translations; and cycle inversions. Rotation moves rotate all rigid body molecular fragments in the cluster by a random angle up to $\pm\pi$ radians; this rotation is about the vector connecting the oxygen

atom of each TIP4P water and the central atom of the tetrahedral ion. Translation moves apply a random displacement to a randomly chosen molecule relative to the rest of the cluster.

The cycle inversion moves are somewhat more complex and involve reducing the hydrogen bonding within the cluster to a network graph in which each water molecule is a node and each hydrogen bond is an edge.[28] This graph is then analyzed, with closed cycles of hydrogen bonds being identified. One of these cycles is then inverted and the graph is then projected back onto the hydrogen bonding network found in the original cluster. In our previous study of sulfate-water clusters, these cycle inversions were found to have a greater effect on total energy for larger hydrogen bonded cycles and to be more beneficial for the global optimization of larger clusters.[11]

The pele software package was used to connect minima on the potential energy landscape for the hydrated perchlorate system. A doubly-nudged elastic band method was used to search for transition states between previously found minima,[29] by sampling between end points using a linear interpolation of the translational coordinates of the rigid-body molecules and spherical linear quaternion interpolation of the rotational coordinates.[30] Candidate transition states were then further optimized using hybrid eigenvector-following.[31,32] The resultant energy landscapes were visualized as disconnectivity graphs using the PyConnect package.[33]

3. Results and Discussion

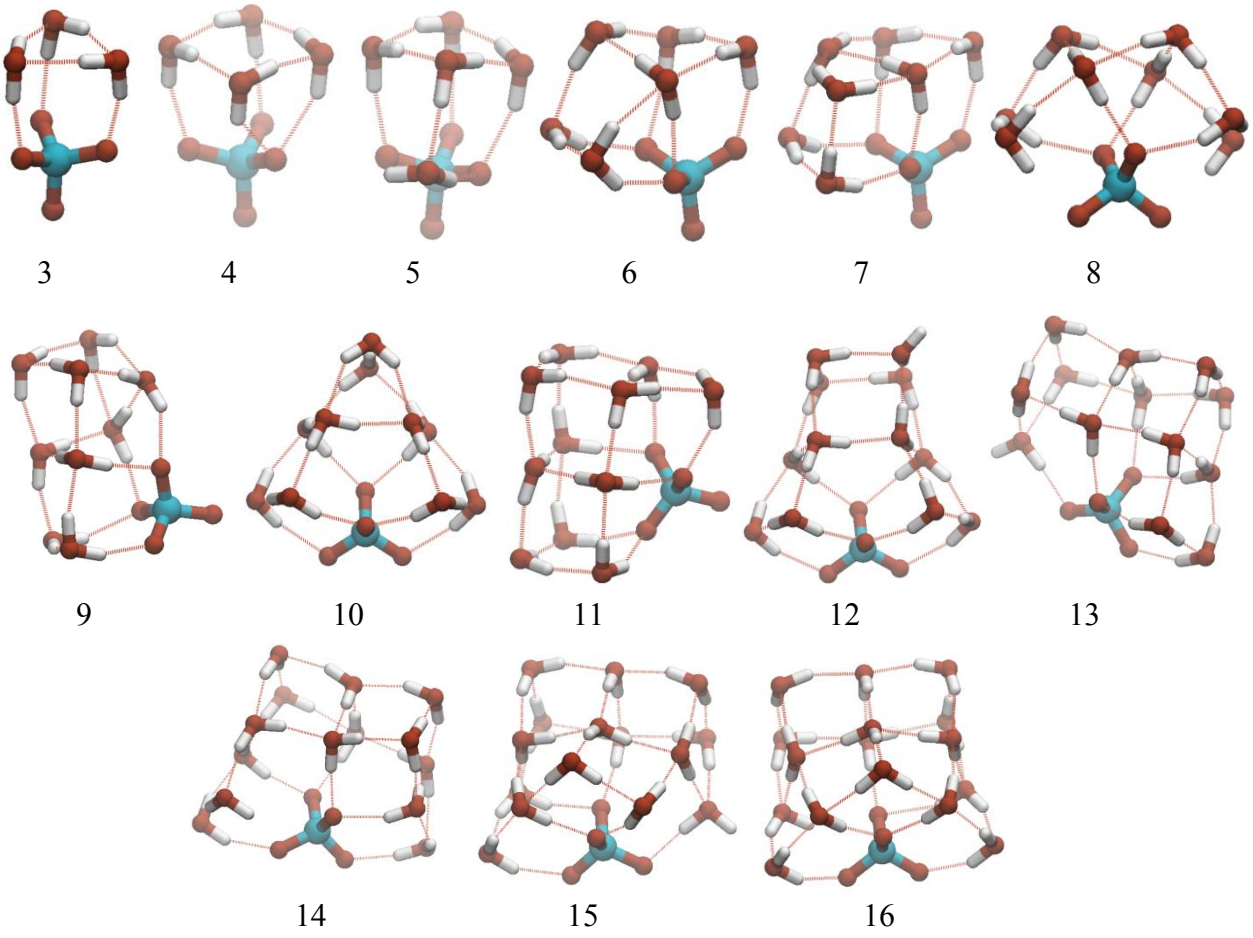

Figure 1. Putative global minimum structures for $\left(ClO_4^-\right)(H_2O)_N$ $3 \leq N \leq 16$.

Eight independent basin-hopping runs were performed for each hydrated perchlorate cluster $\left(ClO_4^-\right)(H_2O)_N$, with $3 \leq N \leq 50$ (to enable comparison with sulfate-water clusters, which are only stable for $N \geq 3$). For perchlorate-water clusters with $N \leq 16$, all of the basin-hopping runs located the same lowest-energy structures, giving us confidence that these are indeed GM. These putative GM are shown in Figure 1 and their interaction energies are listed in Table S1 (Supplementary Material). For clusters with $N > 16$, however, there is a rapid drop off in the number of parallel runs which converge on the same candidate global minimum, with

100% of the runs finding the same minimum at N=16, 63% at N=17 and a maximum of 25% (but often a lower percentage) of runs agreeing for larger sizes.

3.1 Analysis of global minimum structures and energy landscapes for hydrated perchlorate clusters

The structures observed for hydrated perchlorate clusters in this study (see Figure 1) generally have similar structural motifs to those seen in small pure water clusters, i.e. stacked hexagons, pentagons and cubes, albeit in somewhat distorted forms. This distortion is caused by the presence of the perchlorate ion, as it has a smaller effective size than the number of water molecules that it replaces in the pure water cluster. Perchlorate clusters tend to be globular, with low symmetry. The perchlorate ion is usually found on the periphery of the cluster and is not found in the cluster interior even at larger cluster sizes. This is indicative of

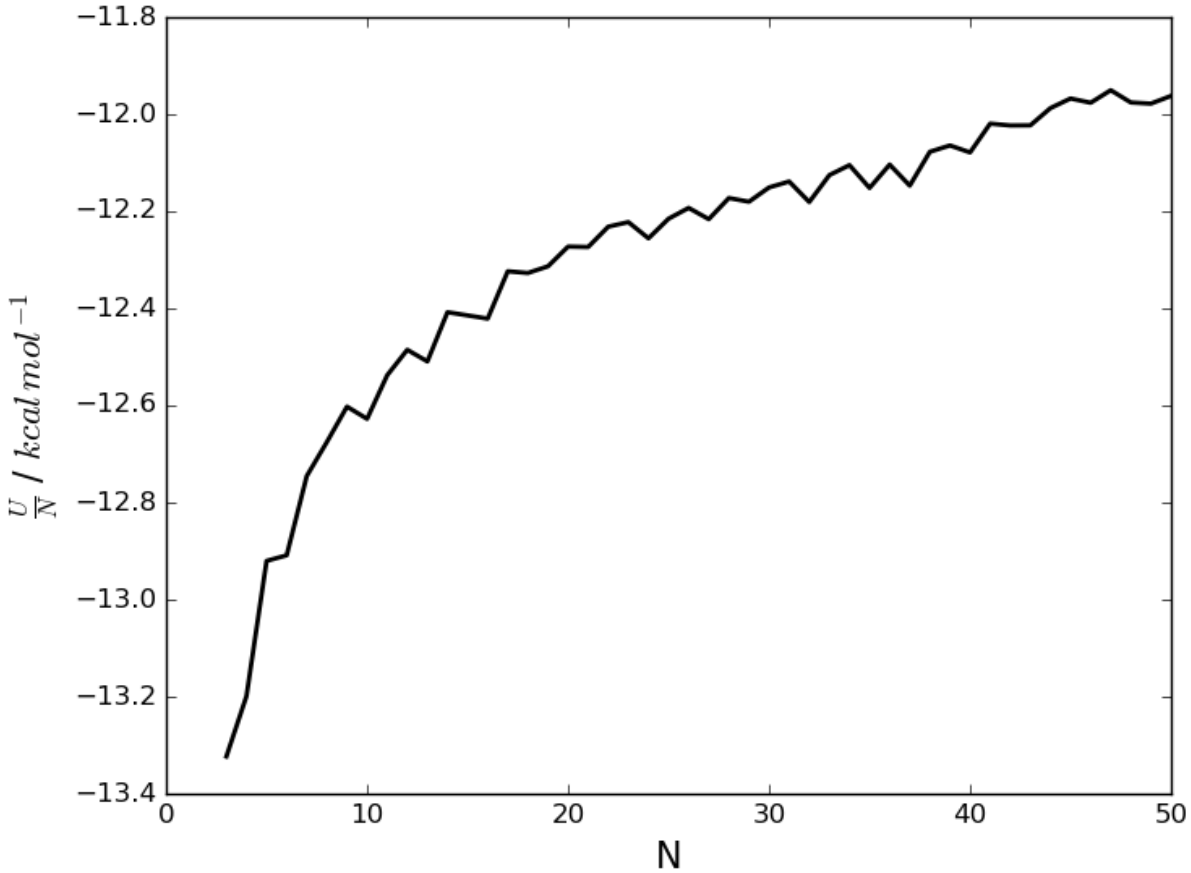

Figure 2. Boltzmann weighted interaction energy per water molecule for the lowest energy minima of $\left(ClO_4^-\right)(H_2O)_N$ for $3 \leq N \leq 50$.

the fact that the water-water hydrogen bonding interactions are the dominant interactions within these clusters.

The evolution of interaction energy per water, shown in Figure 2, demonstrates that 50 water molecules is an insufficient number to have reached the asymptotic limit for bulk TIP4P water, i.e. the infinitely dilute perchlorate solution (≈ -10 kcal mol^{-1}).[34]

3.2 DFT

The 20 lowest energy isomers for each cluster size in the range $3 \leq N \leq 12$ were locally minimized at the density functional theory (DFT) level with the B3LYP exchange-correlation functional and a 6-311++G** basis set, (for consistency with our previous work), as implemented within the NWChem package.[35]

Figure 3 shows the correlation between the DFT and the empirical energy

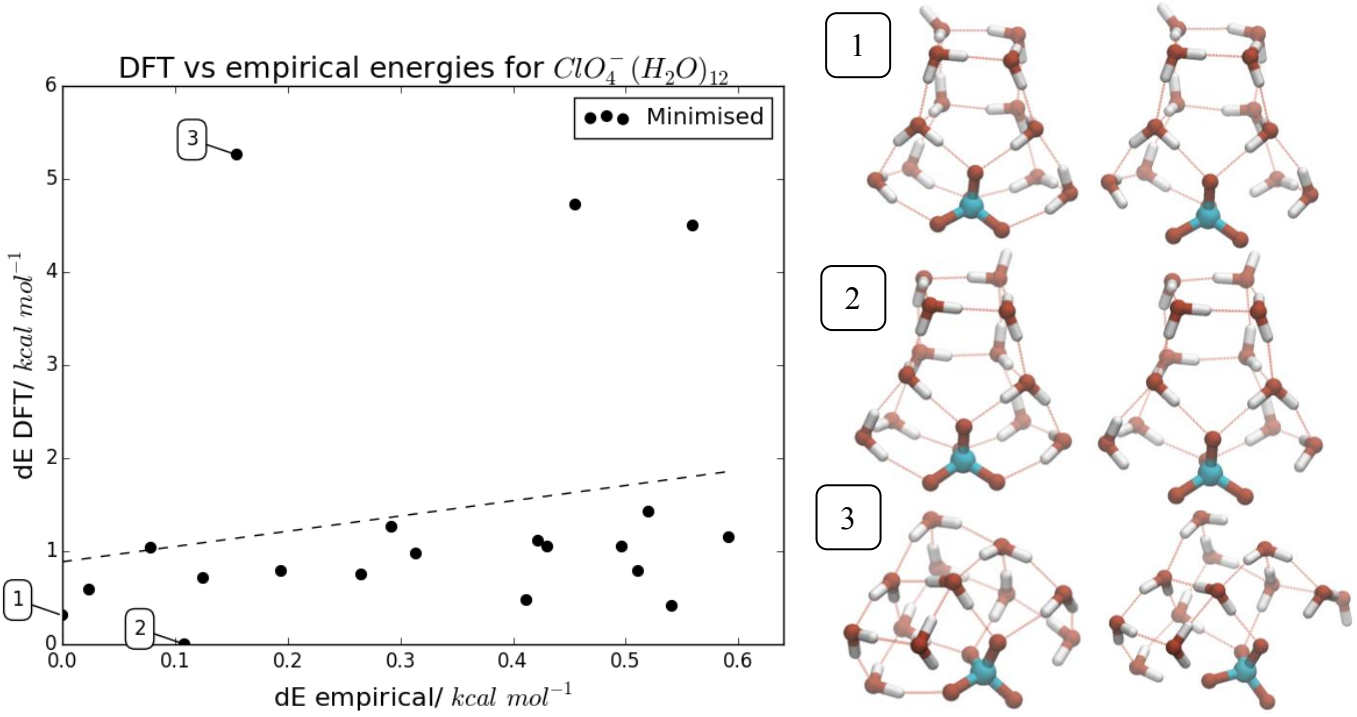

Figure 3. (Left) Locally minimized DFT vs empirical energies for the 20 lowest energy minima found for N=12. Energies are given relative to the respective global minima. And (Right) The corresponding minima found using the empirical model (left) and the structures obtained when these are locally re-minimized at the DFT level (right).

evaluations for the 20 lowest energy $ClO_4^-(H_2O)_{12}$ minima when locally re-minimized at the DFT level. The putative global minimum found at the empirical level, when locally minimized at the DFT level is no longer the global minimum, however this minimum does remain the second most energetically favorable structure. The lowest energy minimum found at the DFT level was identified as the fourth lowest energy minimum at the empirical level. As can be seen in the structures pictured within Figure 3 the empirical and DFT lowest energy minima share the same oxygen framework, with the network of hydrogen bonding being the only significant difference between them. These structures are typical of all of the structures within 1.5 kcal mol^{-1} of the lowest energy structure. Three of the structures re-minimized to be comparatively much less favorable than the others. These structures are all similar in terms of their oxygen frameworks to the labeled structure. Whilst these have all reached local minima, we believe that these are metastable states.

In all of the structures examined there was a general retraction of the water molecules from the ion. This is likely due to the lack of polarization in the model, and would be improved by using a model which accounts for this, such as the AMOEBA forcefield.

3.3 Comparison of global minima of hydrated perchlorate clusters with hydrated sulfate and pure water clusters

There are morphological similarities observed between some of the proposed $(ClO_4^-)(H_2O)_N$ minima and the structures of pure water clusters reported by Wales *et al*.[26] The perchlorate anion tends to take the place of 2-3 water sites within the structure. The presence of the perchlorate ion suppresses dangling OH bonds at the surface by acting as a net acceptor of hydrogen bonds from the coordinated water molecules. This effect can be seen clearly in Figure 4.

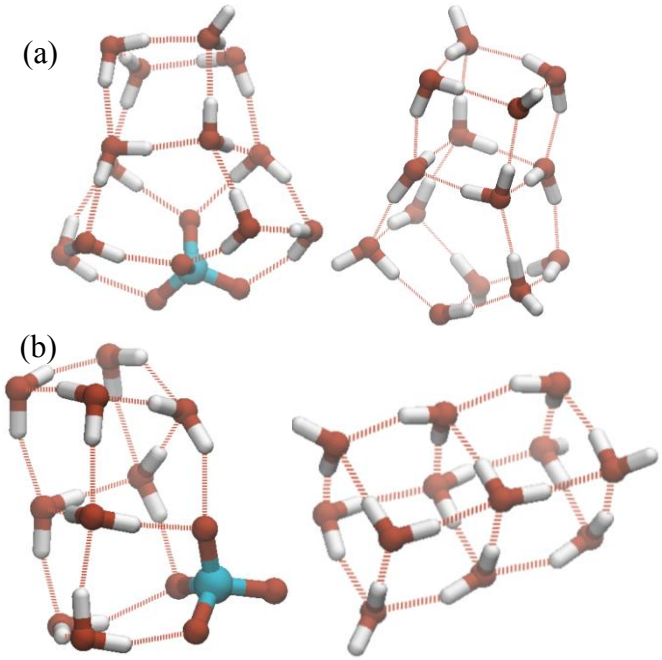

Figure 4. (a) Comparison of $(ClO_4^-)(H_2O)_{12}$ and $(H_2O)_{14}$. (b) Comparison of $(ClO_4^-)(H_2O)_9$ and $(H_2O)_{12}$.

The global minima proposed by Smeeton *et al.* for the hydrated sulfate system share few morphological similarities with the minima proposed for the perchlorate clusters in this study. For sulfate-containing clusters, the ion is almost exclusively located at or near to the center of mass of the cluster, which leads to structures with high symmetry being formed, especially at lower numbers of water molecules ($N < 25$), with examples shown in Figure 5. These high-symmetry structures are almost entirely absent in the minima found for small perchlorate clusters, with the exception of the $(ClO_4^-)(H_2O)_3$ cluster which has the same structure as $(SO_4^{2-})(H_2O)_3$.

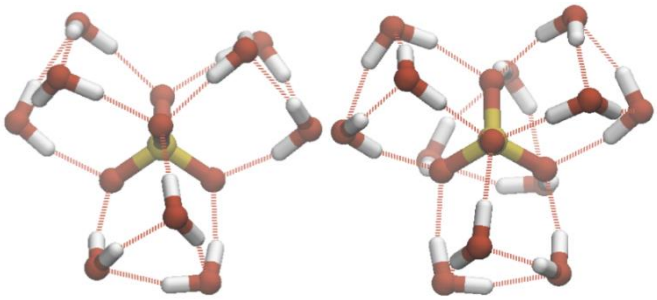

Figure 5. Structures of $(SO_4^{2-})(H_2O)_N$ for N =9 (left) and 12 (right).

3.4 Analysis of dangling OH bonds in hydrated perchlorate and sulfate and pure water clusters

Dangling OH bonds are those which stick out of the surface of the cluster and are not involved in forming hydrogen bonds with other water molecules or the oxyanion. They are of interest because there is experimental data available (due to Williams and co-workers) for the hydrated sulfate system with which we can make comparisons.[11] In the experiment, dangling OH bonds are observed in hydrated sulfate clusters of more than 43 water molecules.[2] This was reproduced computationally in the work conducted by Smeeton *et al*.[11]

The number of dangling OH bonds for the perchlorate system was calculated for each cluster and the Boltzmann weighted mean, (T=130 K), across all the clusters observed was calculated using:

$$\bar{f} = \frac{\sum_i e^{\Delta U_i \beta} f_i}{\sum_i e^{\Delta U_i \beta}} \quad \textbf{(2)}$$

The difference between the energy of cluster i and that of the GM is denoted by ΔU_i, the number of dangling OH bonds is given by f_i, and $\beta = 1/k_B T$. The weighted mean is taken over all structural isomers with unique energies found in all of the basin-hopping runs for each cluster size. A theoretical temperature of 130 K was used to maintain consistency with the previous computational work and the experimental work conducted into hydrated sulfate by Williams and co-workers.[2]

Figure 6 shows a comparison of the Boltzmann weighted mean number of dangling OH bonds as a function of N for hydrated perchlorate and sulfate clusters at T

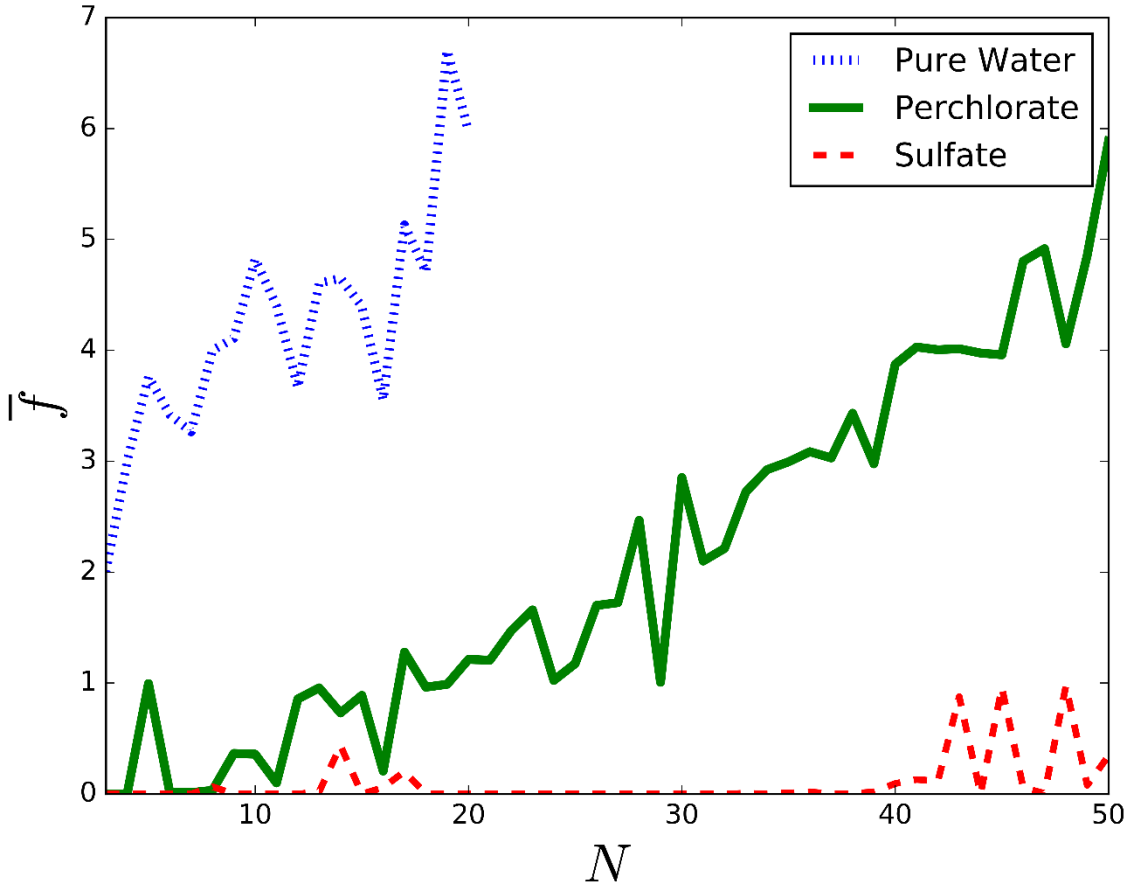

Figure 6. Boltzmann weighted (T = 130 K) mean number of dangling OH bonds ($\bar{f}$) for $(H_2O)_{3\text{-}20}$ and hydrated perchlorate and sulfate clusters with $\mathbf{3 \leq N \leq 50}$ water molecules.

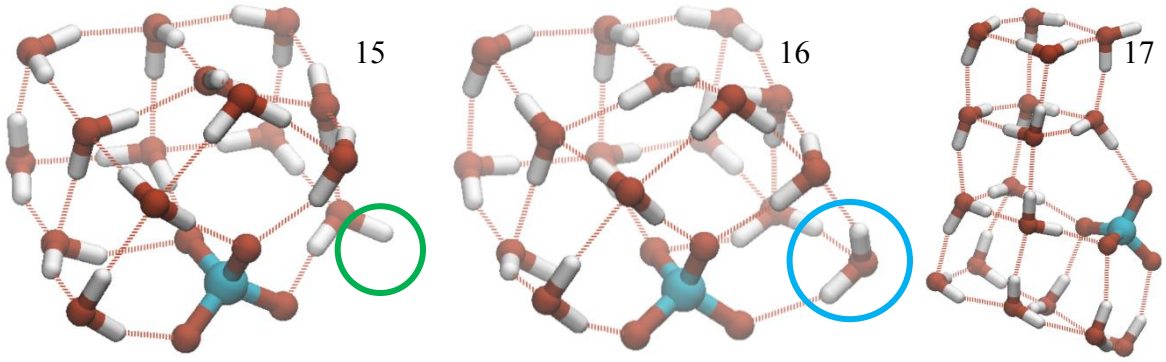

Figure 7. (left to right) lowest energy minima for hydrated perchlorate clusters with N = 15, 16 and 17 water molecules. The unoccupied sites are circled in green and the subsequently filled sites in blue.

= 130 K. Data for pure TIP4P water clusters in the range $3 \leq N \leq 20$ are included for reference. Perchlorate shows a significantly lower incidence of dangling OH bonds than pure water clusters up to N = 20. Across the entire sampled range for perchlorate, an almost total suppression of dangling OH bonds is only seen for N = 3, 6 and 7. None of the candidate GM of $(ClO_4^-)(H_2O)_N$ for N < 12 show dangling OH bonds but higher energy isomers do and it is these which contribute to the non-zero $\bar{f}$ values in the graph. The anomalously low number of dangling OH bonds seen at N = 16 is due to a particularly energetically favorable geometry with very few dangling OHs.

As can be seen in Figure 7, the N=16 perchlorate cluster with anomalously low numbers of dangling OH bonds is closely related in structure to the cluster with one fewer water molecules, with the "additional" water molecule filling in a hole on the cluster surface and interacting with the dangling OH bond (circled in the GM for N = 15) through a hydrogen bond, making the larger cluster more fully saturated. Based upon visual inspection, the minima shown are structurally representative of the 100 lowest minima for each cluster size.

In the work on micro-hydrated sulfate presented by Smeeton *et al.*,[11] the acceptor/donor ratios for hydrogen bonds

exhibited by the water molecules within the system were examined. Water is capable of accepting two hydrogen bonds at the oxygen site, and donating two through the hydrogens. The hydrogen bond acceptor/donor ratio in water systems has an asymptotic limit of 1, but this can never be reached in clusters which exhibit dangling OH bonds. Here, we perform the same analysis for the perchlorate system, plotting the Boltzmann weighted mean acceptor/donor ratio ($\bar{r}_{ad}$) for each cluster size:

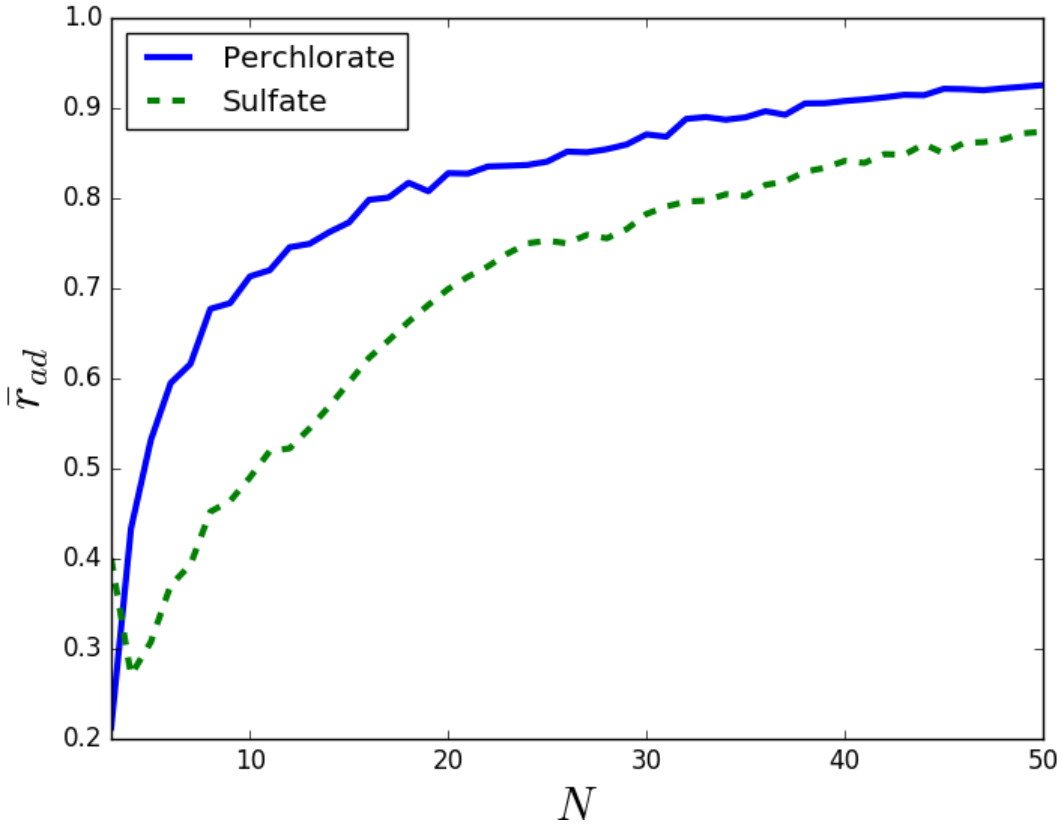

Figure 8. Boltzmann weighted mean acceptor/donor ratios ($\bar{\boldsymbol{r}}_{\boldsymbol{ad}}$) for hydrated perchlorate and sulfate clusters.

$$\bar{r}_{ad} = \frac{\sum_i e^{\Delta U_i \beta} a_i / d_i}{\sum_i e^{\Delta U_i \beta}} \quad \textbf{(3)}$$

where: a_i and d_i are the number of accepted and donated hydrogen bonds on a water molecule in minima i, respectively. Again ΔU_i denotes the energy of cluster i relative to the lowest energy structure and $\beta = 1/k_B T$.

Figure 8 shows a plot of $\bar{r}_{ad}$ for $(ClO_4^-)(H_2O)_N$ and $(SO_4^{2-})(H_2O)_N$ with $3 \leq N \leq 50$. As sulfate generally forms 12-14 hydrogen bonding interactions with water, compared to the 5-6 seen in most perchlorate-water clusters, we expect $\bar{r}_{ad}$ for the water molecules in the cluster to be higher for perchlorate than for sulfate at cluster sizes of N > 3 and this is indeed the case. As neither ion can donate any hydrogen bonds back into the system, they are both net sinks for hydrogen bonding. We observe that at small cluster sizes $\bar{r}_{ad}$ is much larger for perchlorate systems than for sulfate systems: at these sizes sulfate displays a total suppression of dangling OH bonds, whereas perchlorate merely partially suppresses them. At larger cluster sizes $\bar{r}_{ad}$ for the two systems become much closer. At N > 43 dangling OH bonds are reported to reappear in the sulfate-water system. This could be due in part to the outermost water molecules within the clusters falling outside the sphere of influence of the directing effect exerted by the sulfate ion. However, for the perchlorate system there is no significant change in the incidence of dangling OH bonds. For perchlorate $\bar{r}_{ad}$ reaches 0.93 at N = 50, implying that 93% of hydrogen bonds are being accepted by water molecules, for sulfate this is slightly lower at 87%; but in both cases it shows that the clusters are becoming water-like, as the effect of the anion becomes smaller for larger clusters. As the clusters become larger (and the surface/volume ratio decreases) $\bar{r}_{ad}$ should approach the bulk water limiting value of 1.0.

3.5 Comparison of energy landscapes of hydrated perchlorate clusters with hydrated sulfate and pure water clusters

There are significant differences in the energy landscapes obtained for $(ClO_4^-)(H_2O)_N$ and $(SO_4^{2-})(H_2O)_N$, which is demonstrated in Figure 9 for the case of N=8. Our $(H_2O)_8$ disconnectivity graph is

similar in shape to that previously reported by Wales *et al*.[13]

The landscapes obtained for the perchlorate system (Figure 9a) are significantly glassier and frustrated than the landscapes obtained for the sulfate system (Figure 9b). This is to be expected when examining the minima obtained for hydrated perchlorate clusters as they adopt structural features commonly seen in pure water clusters, even at small sizes. This is in stark contrast with the sulfate system (with its preference for more symmetrical structures) which shares very few morphological similarities with water. The landscapes obtained for the sulfate system are more funneled, indicating that there is a stronger directing effect towards the formation of the high symmetry structures observed for sulfate clusters than towards the more asymmetric globular clusters observed for the perchlorate system.

The pure water (TIP4P) disconnectivity graph (Figure 9c) is significantly more frustrated than that of either of the other systems, with large energy barriers separating deep wells ($\geq 3\ kcal\ mol^{-1}$). Frustration is also seen in the disconnectivity graph for the perchlorate system, but to a lesser extent, with smaller barriers separating minima. There is also a deeper funnel present in the perchlorate graph, which suggests a greater directing effect towards the global minimum structure.

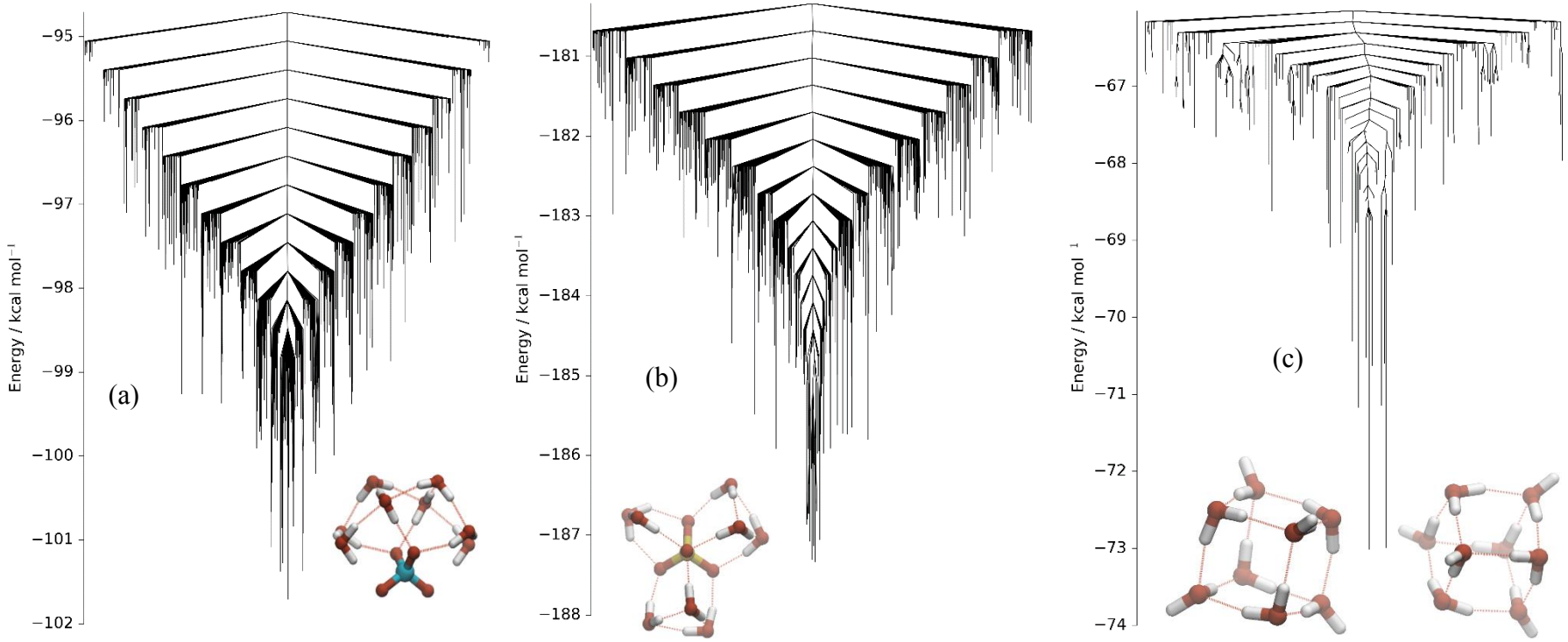

Figure 9. Disconnectivity graphs showing the global minimum and connected minima for the N=8 perchlorate and sulfate ion-water clusters and the pure 8 water cluster. (a) The full landscape for $(ClO_4^-)(H_2O)_8$ comprises 10210 minima and 211152 transition states. (b) The full landscape for $(SO_4^{2-})(H_2O)_8$ comprises similar numbers of minima and transition states. (c) The full landscape for the pure $(H_2O)_8$ cluster comprises 4135 minima and 21270 transition states. Minima are included which are within 7 kcal mol^{-1} of the global minimum

3.6 Investigation of the variation of ion charge

As discussed above, the structures of the GM for hydrated perchlorate and sulfate clusters are quite different. In order to determine to what extent this is due to the charge on the XO_4^q oxyanion, the sulfate interaction energy potential was taken and the overall charge (q) varied in steps of 0.1e from -2.0 (corresponding to sulfate) to -1.0 (perchlorate), while maintaining a constant ratio between the charge on the central atom and on the oxygen, as listed in Table 2. The cluster geometry and the Lennard-Jones parameters were fixed to those for SO_4^{2-}.

Table 2. Partial (q_X, q_O) and overall (q) charges for the central XO_4^q anion in the study of $(XO_4^q)(H_2O)_{12}$.

q_X	q_O	q
+2.4	-1.10	-2.0
+2.28	-1.045	-1.9
+2.16	-0.99	-1.8
+2.04	-0.935	-1.7
+1.92	-0.88	-1.6
+1.80	-0.825	-1.5
+1.68	-0.77	-1.4
+1.56	-0.715	-1.3
+1.44	-0.66	-1.2
+1.32	-0.605	-1.1
+1.20	-0.55	-1.0

The test system chosen to study the effect of charge was $(XO_4^q)(H_2O)_{12}$. As shown in Figure 10, four distinct GM are observed with changing charge q. GM (a) is only observed for q = -2 and corresponds to the previously found GM for $(SO_4^{2-})(H_2O)_{12}$, having three hydrogen-bonded trimer rings sitting symmetrically over the faces of the sulfate tetrahedron, which sits in the center of the cluster. Similarly, GM (d) is only seen for q = -1 and is the same structure previously found as the GM for $(ClO_4^-)(H_2O)_{12}$, consisting of three fused pentagonal prisms. In the interval between q = -2 and -1, there are two intermediate structures, which become more "perchlorate-like" as the total charge approaches -1. GM (b) is the GM for q = -1.9 and -1.8, while

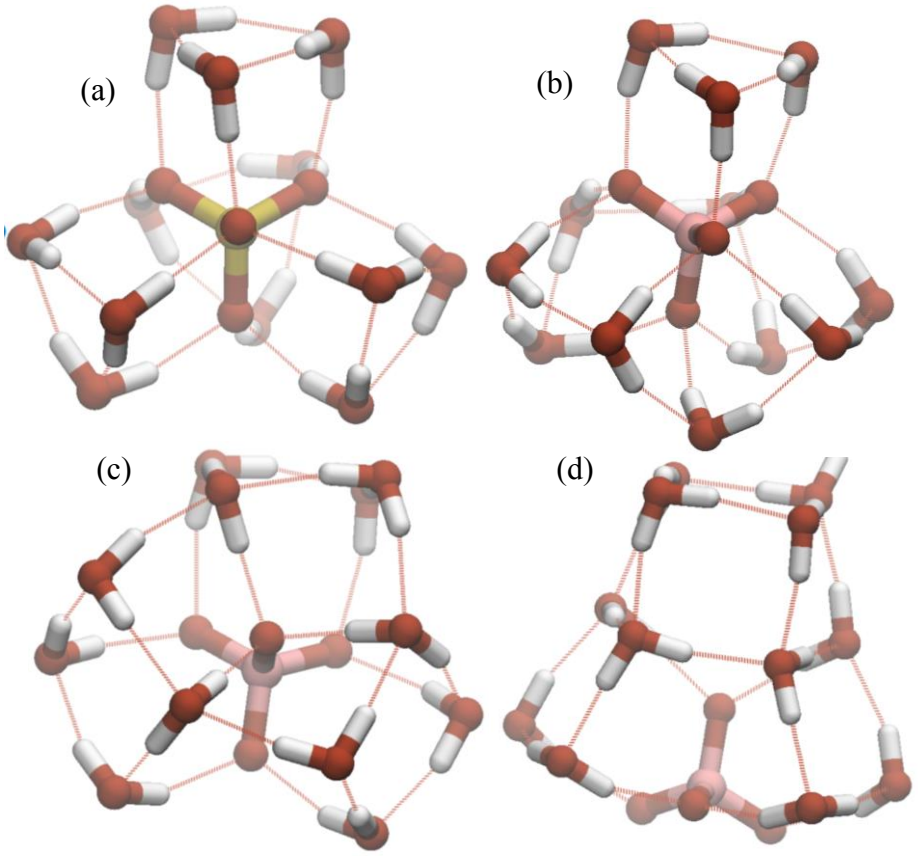

Figure 10. The putative global minima for the variation of total charge (q) in the $(XO_4^q)(H_2O)_{12}$ cluster: (a) q = -2.0; (b) q = -1.9 and -1.8; (c) q = -1.7 to -1.1; (d) q = -1.0.

GM (c) is the GM over a wide range of charges from q = -1.7 to -1.1. Structures (b) and (c) were also observed as competitive structures for $(SO_4^{2-})(H_2O)_{12}$. Structure (b) was found to be the second lowest energy structure of $(SO_4^{2-})(H_2O)_{12}$ with ΔU = 0.6 kcal mol^{-1} and structure (c) being the 59^{th} lowest energy structure found with ΔU = 3.1 kcal mol^{-1}.

The displacement of the heavy atom (X) of

the XO_4^q anion from the geometric centre of the cluster (d_x) is taken as a metric to distinguish between sulfate-like and perchlorate-like clusters, as for the (q = -2) and (q = -1) extremes there is a very clear distinction. As shown in Figure 11, the sulfate-like clusters typically have very low

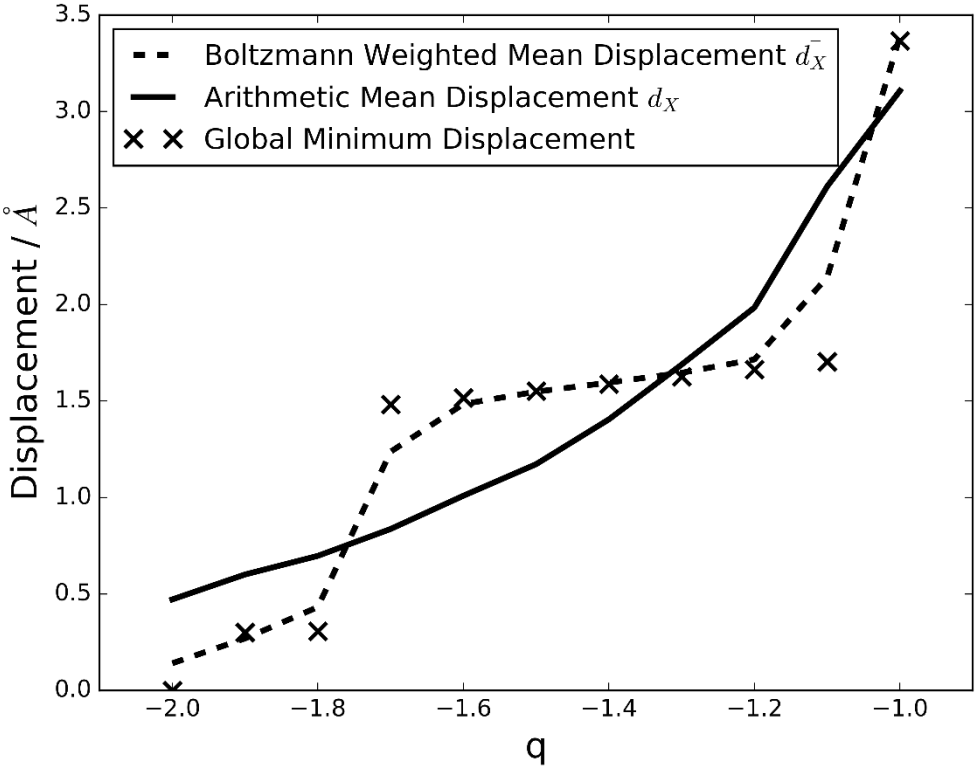

Figure 11. Displacement vs. overall charge (q) for the $(XO_4^q)(H_2O)_{12}$ cluster.

displacements (corresponding to centrally-located sulfate) and the perchlorate clusters

$$\bar{d}_x = \frac{\sum_i e^{\Delta U_i \beta} d_{xi}}{\sum_i e^{\Delta U_i \beta}} \qquad \textbf{(4)}$$

have much higher displacements (corresponding to peripheral perchlorate). When these displacements are taken as the mean over the 100 lowest energy structures which have been found, the increase in displacement approaches the maximum quite smoothly as the charge approaches -1, this is somewhat unexpected as (as shown in Figure 10) there were 4 visually distinct GM for different overall charges but can perhaps be explained by the mixing of higher energy minima. The data were also boltzmann weighted according to:

where d_{xi} is the displacement of X from the geometric centre of cluster i. ΔU_i denotes the energy of cluster i relative to the lowest energy structure and $\beta = 1/k_B T$ (T=130 K). This shows the effect of the four distinct

global minima found at different ranges of charges q. The increasing displacement with decreasing charge is still seen.

4. Conclusions

We have presented candidate global minima for micro-hydrated perchlorate clusters with up to 16 water, using a basin-hopping search strategy and empirical potentials with rigid body molecules. These perchlorate clusters are generally globular in shape, with perchlorate atoms on the periphery of the cluster, and display low-symmetry hydrogen-bonded cages which are commonly seen in pure water clusters. There are no clusters with N > 3 for which perchlorate adopts the same lowest energy structure as previously reported for sulfate-water clusters.[11]

The total suppression of dangling OH bonds, seen both experimentally and computationally for the sulfate-water system, is not present in the perchlorate-water system for any cluster with more than eight water molecules, although there is a significantly lower incidence of dangling OH bonds when compared with pure water clusters of up to 20 molecules.

The energy landscapes produced for the perchlorate-water clusters show significant frustration, with comparatively large energy barriers connecting several different low energy structures. These energy landscapes show significant parallels with those obtained for pure water clusters, as both are highly frustrated. The significant directing effect towards a small number of low energy minima which is observed for the sulfate-water clusters is not seen in the perchlorate system, although there is a smaller directing effect present which is greater than that seen in the energy landscapes of pure water clusters.

Hydrated perchlorate and sulfate clusters and pure water clusters behave quite differently and there are clear differences in the observed structures of the low-energy

minima for the hydrated perchlorate and sulfate clusters, as well as the pure water clusters. The sulfate system favors high-symmetry structures, whilst the perchlorate and pure water systems typically adopt lower-symmetry structures. The perchlorate ion favors sites on the surface the cluster, whilst the sulfate occupies the center of the cluster. This is due to the water-water hydrogen bonding interactions being dominant in determining the morphology of the $(ClO_4^-)(H_2O)_N$ clusters: placing perchlorate at the surface maximizes the total number of water-water interactions, consistent with partial solvation of the singly charged anion. The opposite is true in the sulfate system, where (due to the higher ionic charge) maximization of the number of water-ion interactions is favored.

The clear charge dependence of the adopted geometries of the solvated ions was again observed in the varied-charge investigation. With a perchlorate like monoanion, the observed global minimum energy structure was the same as that proposed for perchlorate, and this structure had the ion on the cluster surface. As the charge on the ion was increased the ion gradually migrated towards the center of the cluster, until the dianion was located at the geometric center of the cluster. This suggests that charge, or charge density, is the dominant factor in determining the observed morphologies of hydrated Hofmeister ion clusters as, despite significant difference in the Lennard-Jones parameters used for the perchlorate and sulfate anions, the hypothetical $(SO_4^-)(H_2O)_{12}$ cluster adopted the same structure as $(ClO_4^-)(H_2O)_{12}$.

Supplementary Information

Table S1 contains the energies for all of the reported putative global minima.

Copies of all the structures analyzed in this work, as well as a copy of the basin hopping code used to generate them, will be

made publicly available through the Research Data Archive service at Birmingham.

Acknowledgements

We acknowledge the Engineering and Physical Sciences Research Council, UK (EPSRC), for funding under Program Grant EP/I001352/1. Computational facilities were provided by the MidPlus Regional Centre of Excellence for Computational Science, Engineering and Mathematics, under EPSRC Grant EP/K000128/1 and the University of Birmingham's BlueBEAR HPC service, which provides a High-Performance Computing service to the University's research community (see http://www.birmingham.ac.uk/bear for more details). The authors would also like to thank Dr. Sven Heiles and Prof. Evan Williams (U.C. Berkeley) for their experimental input and helpful comments.

References

(1) Xie, W. J.; Gao, Y. Q. A Simple Theory for the Hofmeister Series. *J. Phys. Chem. Lett.* **2013**, *4* (24), 4247–4252.

(2) Obrien, J. T.; Prell, J. S.; Bush, M. F.; Williams, E. R. Sulfate Ion Patterns Water at Long Distance. *J. Am. Chem. Soc.* **2010**, *132* (24), 8248–8249.

(3) Cacace, M. G.; Landau, E. M.; Ramsden, J. J. The Hofmeister Series: Salt and Solvent Effects on Interfacial Phenomena. *Q. Rev. Biophys.* **1997**, *30*, 241–277.

(4) Baer, M. D.; Kuo, I.-F. W.; Bluhm, H.; Ghosal, S. Interfacial Behavior of Perchlorate versus Chloride Ions in Aqueous Solutions. *J. Phys. Chem. B* **2009**, *113* (48), 15843–15850.

(5) dos Santos, A. P.; Levin, Y. Surface and Interfacial Tensions of Hofmeister Electrolytes. *Faraday Discuss.* **2013**, *160* (0), 75–87.

(6) Pokorná, J.; Heyda, J.; Konvalinka, J. Ion Specific Effects of Alkali Cations on the Catalytic Activity of HIV-1 Protease. *Faraday Discuss.* **2013**, *160* (0), 359–370.

(7) Tobias, D. J.; Stern, A. C.; Baer, M. D.; Mundy, C. J. Atmospherically Relevant Aqueous Liquid-Air Interfaces. 1–53.

(8) Light, T. P.; Corbett, K. M.; Metrick, M. A.; Macdonald, G. Hofmeister Ion-Induced Changes in Water Structure Correlate with Changes in Solvation of an Aggregated Protein Complex. **2016**.

(9) Eisenberg, B. Ionic Interactions in Biological and Physical Systems: A Variational Treatment. *Faraday Discuss.* **2013**, *160* (0), 279–296.

(10) Kunz, W. Specific Ion Effects in Colloidal and Biological Systems. *Curr. Opin. Colloid Interface Sci.* **2010**, *15*, 34–39.

(11) Smeeton, L. C.; Farrell, J. D.; Oakley, M. T.; Wales, D. J.; Johnston, R. L. Structures and Energy Landscapes of Hydrated Sulfate Clusters. *J. Chem. Theory Comput.* **2015**, *11* (5), 2377–2384.

(12) Rühle, V.; Kusumaatmaja, H.; Chakrabarti, D.; Wales, D. J. Exploring Energy Landscapes: Metrics, Pathways, and Normal-Mode Analysis for Rigid-Body Molecules. *J. Chem. Theory Comput.* **2013**, *9*, 4026–4034.

(13) Chakrabarti, D.; Wales, D. J. Simulations of Rigid Bodies in an Angle-Axis Framework. *Phys. Chem. Chem. Phys.* **2009**, *11* (12), 1970–1976.

(14) Heinje, G.; Luck, W. P.; Heinzinger, K. Molecular Dynamics Simulation of Aqueous NaClO4 Solution. *J. Phys. Chem.* **1987**, *91* (4), 331–338.

(15) Wagner, E. L. Bond Character in XYM-Type Molecules: Chlorine—Oxygen Compounds. *J. Chem. Phys.* **1962**, *37* (4), 751.

(16) Cannon, W. R.; Pettitt, B. M.; Mccammont, J. A. Sulfate Anion in Water : Model Structural , Thermodynamic , and Dynamic Properties. *J. Phys. Chem.* **1994**, *98*, 6225–6230.

(17) Kazachenko, S.; Thakkar, A. J. Water Nanodroplets: Predictions of Five Model Potentials. *J. Chem. Phys.* **2013**, *138* (19), 194302–194310.

(18) Jorgensen, W. L.; Chandrasekhar, J.; Madura, J. D.; Impey, R. W.; Klein, M. L. Comparison of Simple Potential Functions for Simulating Liquid Water. *J. Chem. Phys.* **1983**, *79* (2), 926.

(19) Kazachenko, S.; Thakkar, A. J. Improved Minima-Hopping. TIP4P Water Clusters, (H2O)(n) with N<= 37. *Chem. Phys. Lett.* **2009**, *476* (1–3), 120–124.

(20) Sanz, E.; Vega, C.; Abascal, J. L. F.; MacDowell, L. G. Tracing the Phase Diagram of the Four-Site Water Potential (TIP4P). *J. Chem. Phys.* **2004**, *121* (2), 1165–1166.

(21) Sanz, E.; Vega, C.; Abascal, J. L. F.; MacDowell, L. G. Phase Diagram of Water from Computer Simulation. *Phys. Rev. Lett.* **2004**, *92* (25).

(22) Wales, D. J.; Doye, J. Global Optimization by Basin-Hopping and the Lowest Energy Structures of Lennard-Jones Clusters Containing up to 110 Atoms. *J. Phys. Chem. A* **1997**, *93* (24), 5111–5116.

(23) LI, Z. Q.; SCHERAGA, H. A. Monte-Carlo Minimization Approach to the Multiple-Minima Problem in Protein Folding. *Proc. Natl. Acad. Sci. U. S. A.* **1987**, *84* (19), 6611–6615.

(24) Wales, D. J.; Scheraga, H. A. Review: Chemistry - Global Optimization of Clusters, Crystals, and Biomolecules. *Science (80-.).* **1999**, *285* (5432), 1368–1372.

(25) *Python Energy Landscape Explorer: Http://pele-Python.github.io/pele/ Accessed on: 03/12/2015*.

(26) Wales, D. J.; Hodges, M. P. Global Minima of Water Clusters (H2O)n, n≤21, Described by an Empirical Potential. *Chem. Phys. Lett.* **1998**, *286* (April), 65–72.

(27) Kato, M.; Uchida, T.; Matsumoto, T.; Sunaoshi, T.; Nakamura, H.; Machida, M. Thermal Expansion Measurement and Heat Capacity Evaluation of Hypo-Stoichiometric PuO2.00. *J. Nucl. Mater.* **2014**, *451* (1-3), 78–81.

(28) Takeuchi, H. Development of an Efficient Geometry Optimization Method for Water Clusters. *J. Chem.*

Inf. Model. **2008**, *48* (11), 2226–2233.

(29) Trygubenko, S. A.; Wales, D. J. A Doubly Nudged Elastic Band Method for Finding Transition States. *J. Chem. Phys.* **2004**, *120* (5), 2082–2094.

(30) Shoemake, K. Animating Rotation with Quaternion Curves. *ACM SIGGRAPH Comput. Graph.* **1985**, *19*, 245–254.

(31) Henkelman, G.; Jonsson, H. A Dimer Method for Finding Saddle Points on High Dimensional Potential Surfaces Using Only First Derivatives. *J. Chem. Phys.* **1999**, *111* (15), 7010–7022.

(32) Munro, L. J.; Wales, D. J. Defect Migration in Crystalline Silicon. *Phys. Rev. B* **1999**, *59* (6), 3969–3980.

(33) Smeeton, L. C.; Oakley, M. T.; Johnston, R. L. Visualizing Energy Landscapes with Metric Disconnectivity Graphs. *J. Comput. Chem.* **2014**, *35* (20), 1481–1490.

(34) Jorgensen, W. L.; Madura, J. D. Temperature and Size Dependence for Monte-Carlo Simulations of TIP4P Water. *Mol. Phys.* **1985**, *56* (6), 1381–1392.

(35) Valiev, M.; Bylaska, E. J.; Govind, N.; Kowalski, K.; Straatsma, T. P.; Dam, H. J. J. Van; Wang, D.; Nieplocha, J.; Apra, E.; Windus, T. L.; et al. NWChem : A Comprehensive and Scalable Open-Source Solution for Large Scale Molecular Simulations ☆. *Comput. Phys. Commun.* **2010**, *181* (9), 1477–1489.

TOC Graphic: